Original Article

Thai Journal of Pharmaceutical Sciences

In silico evaluation of molecular interactions between known α-glucosidase inhibitors and homologous α-glucosidase enzymes from *Saccharomyces cerevisiae, Rattus norvegicus,* and GANC-human

Teni Ernawati[1,2], Abdul Mun'im[1], Muhamad Hanafi[2], Arry Yanuar[1]

[1]Department of Pharmaceutical Sciences, Faculty of Pharmacy, Universitas Indonesia, Depok 16242, Indonesia, [2]Medicinal Chemistry Division, Research Center for Chemistry, Indonesian Institute of Sciences (LIPI), Kawasan Puspiptek, Serpong Tangerang Selatan, Banten 15314, Indonesia

Corresponding author:
Arry Yanuar, Department of Pharmaceutical Sciences, Faculty of Pharmacy, Universitas Indonesia, Depok 16242, Indonesia.
E-mail: arry.yanuar@ui.ac.id

Received: Apr 06, 2017
Accepted: Dec 12, 2017
Published: Jan 10, 2018

Keywords:
Human (GANC) α-glucosidase enzyme, molecular docking, *Rattus norvegicus, Saccharomyces cerevisiae*, α-glucosidase

ABSTRACT

The aim of this study was to observe molecular interactions between α-glucosidase inhibitor (IAG) and α-glucosidase enzymes derived from Saccharomyces cerevisiae, Rattus norvegicus, and GANC-human. These enzymes were studied against four of the well-known IAG such as 1-deoxynojirimycin, acarbose, miglitol, and voglibose. We compared the selected IAG by means of a computer-aided drug design protocol involving homology modeling of the target protein and the virtual screening with docking simulations in the binding free energy function. Compared to acarbose, miglitol, voglibose, 1-deoxynojirimycin showed a significant inhibition of three target macromolecules of α-glucosidase enzyme. 1-Deoxynojirimycin had the highest inhibition on α-glucosidase, followed by miglitol, voglibose, and acarbose, respectively.

INTRODUCTION

α-Glucosidase enzyme is a type of hydrolase enzyme that catalyzes the hydrolysis of non-reducing terminal carbohydrates into α-glucose.[1] Carbohydrates are digested by enzymes in the mouth and intestines into simpler sugars which are then absorbed into the body, and hence, they increase the blood sugar levels. With the rejection of the α-glucosidase enzyme, glucose levels in the blood could be returned within the normal limits.[2] Glucosidase is responsible for the catalytic cracking of glycosidic bonds specifically depending on the number of monosaccharide, the position of the cleavage site, and the configuration of the hydroxyl group in the substrate.[3] The main mechanism of the enzymatic hydrolysis of glycosidic bonds was proposed by Koshland through the mechanism of detention and inversion in anomeric configuration.[4] Inhibition of the α-glucosidase enzyme causes inhibition of glucose absorption. Compounds that can inhibit α-glucosidase enzyme called α-glucosidase inhibitors (IAG). IAG compounds are widely used for the treatment of type 2 diabetes.[5] There are many α-glucosidase enzyme inhibitors that have been reported such as acarbose, nojirimycin, 1-deoxynojirimycin,[6] miglitol,[2] and voglibose.[7] IAG prevents α-glucosidase enzyme in the intestinal wall. The α-glucosidase enzymes such as maltase, isomaltase, and glucomaltase serve to hydrolyze the oligosaccharides

on the intestinal wall. The clinical uses of IAG are not only for treatment of obesity and diabetes but also they can also be used as therapeutic targets for some diseases, which are affected by carbohydrate level such as viral infections,[8] anti-HIV,[9] anti-tumor,[10] hepatitis,[8] and syndrome metabolic.[11]

In this study, we analyzed molecular modeling studies of the known IAG such as 1-deoxynojirimycin, acarbose, miglitol, and voglibose against three protein models. The molecular docking simulation involves homology modeling and ligand-based virtual screening. Ligand-based virtual screening approach was employed to calculate the lowest binding energy between the α-glucosidase enzymes with a ligand. We chose three of the α-glucosidase enzymes derived from baker's yeast *Saccharomyces cerevisiae*, *Rattus norvegicus,* and GANC-human as the target proteins in the virtual screening because they are the well-known molecular templates for evaluating and searching for IAG.[6,12-15] When assaying the activity of a compound, the activity might be affected by species difference. Specifically, in α-glucosidase assay, species difference would produce different results. The common testing of IAG was carried out on *S. cerevisiae* and mammalian α-glucosidase, while the main target was human α-glucosidase. These species-based differences in the inhibitory activities of the known IAG should be investigated to increase our understanding of the structure-activity relationship. In this study, the species difference with regard to the inhibitory activity of these compounds had been examined by a computational method.[16] This computational study method could be used as a reference to determine the prediction of IAG activity from three existing species.

MATERIALS AND METHODS

The 2D and 3D structures of 1-deoxynojirimycin, acarbose, miglitol, and voglibose compounds were drawn by Marvin Sketch and ChemDraw 12.0 [Figure 1]. The experiment was performed on a computer with Intel Core i5 −4460 processor (3.20 GHz) and the Windows 7 Ultimate as the operating system. Software used in this work included the application tethering molecules using Autodock 4.2, the homology modeling template using SWISS-MODEL, application of molecular visualization using UCSF-Chimera 1.9, and Autodock 4.2 RAMPAGE for testing Ramachandran plot.

Homology modeling of *S. cerevisiae, R. norvegicus*, and GANC-human α-glucosidase: 3D structure generation using computational methods

The target protein to be used was α-glucosidase derived from *S. cereviseae*. This protein was not yet available at the website of Protein Data Bank (PDB). Therefore, we searched for a target protein in GeneBank sequence database. This database was created by the National Center for Biotechnology Information. We chose the corresponding protein to be made using Swiss-Model homology with existing mold in the PDB; it could be accessed at www.pdb.org. For the target protein, first, we chose UniprotKB/Swiss-Prot: P53051.1. Then, we made homology of the model with existing mold on GDP (PDB ID: 3axh.1.A). Model template made by Swiss-Model had a similarity sequence identity of 99.83%. Furthermore, our model superposed with 3axh.1.A uses Chimera. To assess the overall stereochemical quality of protein analysis, Ramachandran plot of the model was conducted using RAMPAGE program.

The target protein to be used was α-glucosidase derived from *R. norvegicus*. For this target protein, we chose UniprotKB/Swiss-Prot: D3ZTX4_RAT. Then, we made homology of the model with existing mold on GDP (PDB ID: 3l4×.1.A). Model template made by Swiss-Model had a similarity sequence identity of 82.91%. Furthermore, our model was superposed using Chimera. To assess the overall stereochemical quality of protein analysis, Ramachandran plot of the model was conducted using RAMPAGE program.

The target protein to be used was α-glucosidase derived from GANC-human. The target protein from GANC-human

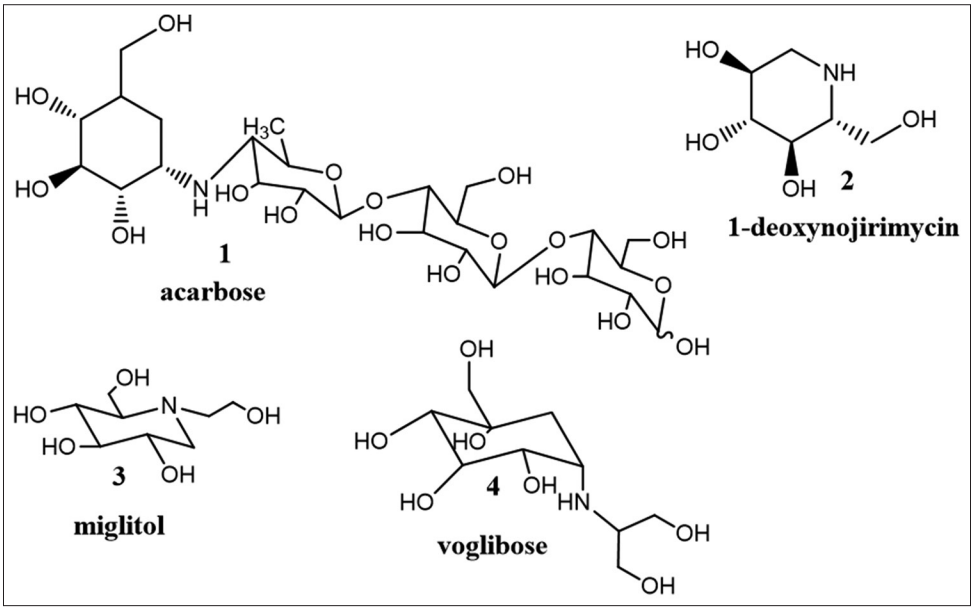

Figure 1: Chemical Structures of the α-glucosidase inhibitors; acarbose (1), 1-deoxynojirimycin (2), miglitol (3), voglibose (4)

was used by the crystal structure of α-glucosidase. The process involves homology modeling of α-glucosidase C-neutral human beings (GANC) with 914 amino acid residues from the Swiss-Prot with Q8TET4 identity and the template mold 2G3M. Model template made by Swiss-Model had a similarity sequence identity of 31.35%.

Validation Docking Simulations

Validation was done by comparing the value of the bond between the active ligand and ligand receptor by ligand binding site that compares receptor-ligand binding site. Analysis of the data was revealed by rate mean square deviation (RMSD) value ratio (RMSD). Docking method is said to be good if its RMSD value is ≤2.0. If the RMSD value is >2.0, then the method used cannot be trusted.

Optimization of Macromolecules

Macromolecules that have been superposed were prepared for tethering. Macromolecules were optimized using software Autodock 4.2. 3D structure of macromolecules was added with hydrogen atoms. Next, their charges were repaired by adding the partial charges of Gasteiger charges. Finally, they were given force field of Autodock.

Molecular Docking Simulation[17]

First, macromolecular and ligand structure to be tethered were optimized. Next, PDBQT files were created for both macromolecule and ligand. Furthermore, grid parameter file (GPF) and docking parameter file (DPF) were created. GPF would inform Autogrid about potential receptors that need to be calculated and the type of map that must be counted and its location. A grid box of the protein structure was then generated using Autogrid 4 software with X, Y, and Z for *S. cerevisiae, R. norvegicus,* and GANC human. They were −20.22, −5.33, and −22.22; 2.17, −19.98, and 20.23; and −21.72, −6.32, and −5.28, respectively, volume grid 50 × 50 × 50 Å, grid spacing of 0.375 Å. While the DPF would inform Autodock about the map that would be used, the ligand to be moved, including the center and the torque of the ligand, docking algorithm to be used, and the number of docking to be done.

RESULTS AND DISCUSSION

Most of the biological testing of IAG was carried out on *S. Cerevisiae;* however, rat intestinal was actually the better choice since it has similar genetic sequence to the human's. To understand the mechanism of ligand binding and to identify potent inhibitors, we ran molecular docking using three protein models. The goal of this research was to observe molecular interactions between IAG with α-glucosidase enzyme derived from *S. cerevisiae, R. norvegicus*, and GANC-human.

Molecular modeling studies of the known inhibitors were conducted to determine the specific interaction between the known the IAG (compounds 1-4, Figure 1) with the variety of macromolecule targets. This research was done instead because there are limitations on doing experiment directly on human. The actual glucosidase target should have been glucosidase from human. Many biological activity tests were done using *S. cerevisiae* and intestinal rat.[18-21] To clarify the binding site and the inhibitory mechanism of the these three protein models, the homology proteins were calculated and their 3D structures were shown in Figure 2**.**

The structure of *S. cerevisiae* oligo-1.6-glucosidase IMA1 3axh.1.A was taken as a template for showing similarity of 99.83%. Selected target sequences were α-glucosidase derived from yeast *S. cerevisiae* with 589 amino acid residues taken from Uni-Prot with P53051.1. The crystal of 3axh.1. A was completed with the crystal structure of isomaltase of *S. cerevisiae* which had a resolution of 1.8 Å. For a selected target sequence, α-glucosidase was derived from *R. norvegicus* with 1795 amino acid residues taken from Uni-Prot with D3ZTX4_RAT identity. In this homology modeling, molds were taken from GDP with the code PDB ID: 3l4x.1.A. Crystals of 3l4x.1.A were maltase-glucoamylase complex N-terminal human being which had a resolution of 1.9 Å with similarity sequence identity of 82.91%. This protein consisted of 868 amino acid residues. While the target macromolecules were used by the crystal structure of α-glucosidase which involved in homology modeling of C-neutral human beings (GANC), α-glucosidase with 914 amino acid residues derived from Uni-Prot with Q8TET4 identity and using the template mold 2G3M with similarity sequence identity of 31.35%. Although similarity sequence identity was quite low, the evaluation of the homology model indicated that this model was still within a usable range and also supported by a RMSD value of 1.458

Table 1: Ramachandran plot statistic for the *S. cerevisiae, R. norvegicus*, and GANC-human model

Model of α-glucosidase	Distribution of residual regions	α residue (%)
S. cerevisiae	Residues in most favored regions	573 (98.1)
		11 (1.9)
	Residues in allowed regions	0 (0)
	Residues in outlier regions	
R. norvegicus	Residues in most favored regions	826 (96.3)
		32 (3.7)
	Residues in allowed regions	0 (0)
	Residues in outlier regions	
GANC-human	Residues in most favored regions	391 (88.5)
		48 (10.9)
	Residues in allowed regions	3 (0.7)
	Residues in outlier regions	

S. cerevisiae: Saccharomyces cerevisiae, R. norvegicus: Rattus norvegicus

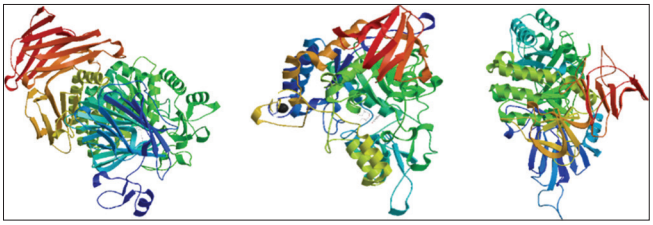

Figure 2: Ribbon diagrams of the template structure of the α-glucosidase the homology modeled structure; (a) *Saccharomyces cerevisiae*, (b) *Rattus norvegicus*, *(c)* GANC-human

Table 2: Result of docking scores of IAG

IAG	Result of Docking								
	S. cerevisiae			*R. norvegicus*			GANC human		
	ΔG (kcal/mol)	Ki (μM)	H-bond	ΔG (kcal/mol)	Ki (μM)	H-bond	ΔG (kcal/mol)	Ki (μM)	H-bond
Acarbose (1)	3.55	-	5	−6.12	32.64	6	−2.88	7.77	3
1-Deoxynojirimycin (2)	−6.57	15.38	3	−5.93	45.36	5	−6.07	35.53	7
Miglitol (3)	−4.54	466.71	5	−4.37	262.62	7	−5.04	201.15	6
Voglibose (4)	−4.21	823.99	7	−3.96	1.26	5	−3.55	2.50	5

S. cerevisiae: Saccharomyces cerevisiae, R. norvegicus: Rattus norvegicus

Å. To predict the accuracy of the protein-ligand docking on the homology model, Ramachandran statistical plots were used. Ramachandran plots of *S. Cerevisiae, R. Norvegicus,* and GANC-human showed normal distribution of points with phi (α) values and psi (ψ) values clustered in a few distinct regions of residues occupying core and allowed regions, respectively, as presented in Table 1.

Binding mode of the inhibitor was the main factor in the prediction of the binding affinity. Each structure of the known IAG bound to the catalytic domain was constructed by superposition of the crystal structures. Binding affinity between each ligand and enzyme domain was calculated. Calculated binding affinities of the known IAG for each domain were summarized in Table 2. All the known IAG were docked into the binding pocket of homology modeling of α-glucosidase enzyme. From the results of molecular docking, it was considered that the top-ranked conformation of the most active among three protein models is 1-deoxynojirimycin. 1-deoxynojirimycin showed a significant inhibition of three target macromolecule of α-glucosidase enzyme. This can be seen from the relatively highest ΔG and Ki values in *S. cerevisiae* (−6.57 kcal/mol, 15.38 μM) and GANC macromolecules (−6.07 kcal/mol, 35.53 μM) except for macromolecule of *R. norvegicus*, 1-deoxynojirimycin (−5.93 kcal/mol, 45.36 μM) occupying the second position after acarbose (−6.12 kcal/mol, 32.64 μM). The difference in value was not large, so it could be considered the same as having a quite good value in the receptor. Acarbose has the best ΔG value in *R. norvegicus* (rat), then it was relatively good in humans but not good for *S. cerevisiae* (yeast). Inhibition activity at rat was 3 times higher than in humans.[22] Acarbose showed poor inhibition in *S. cerevisiae* since it was possible that the mechanism of action of α-glucosidase enzymes in yeast, rat, and humans had different working mechanisms.

Docking simulation not only presented an understanding of the binding mode of the ligands but it was also employed to validate the homology model. The interactions of the *S. cereviseae* α-glucosidase and 1-deoxynojirimycin proposed in this study were useful to understand the potential mechanisms of the interaction between *S. cereviseae* and 1-deoxynojirimycin. The residues of Asp69, Asp352, and Arg442 were important for strong hydrogen bonding interaction with 1-deoxynojirimycin, as shown in Figure 3. Acarbose had been known as IAG and used as antidiabetic drugs. However, the inhibitory activity of acarbose on α-glucosidase of *S. cerevisiae* was not good. To test IAG on *S. cerevisiae,* it was not suitable to use acarbose as a standard reference for glucosidase inhibitor. Miglitol and voglibose were considered as moderate IAG and had bonding interaction with α-glucosidase *S. cerevisiae*.

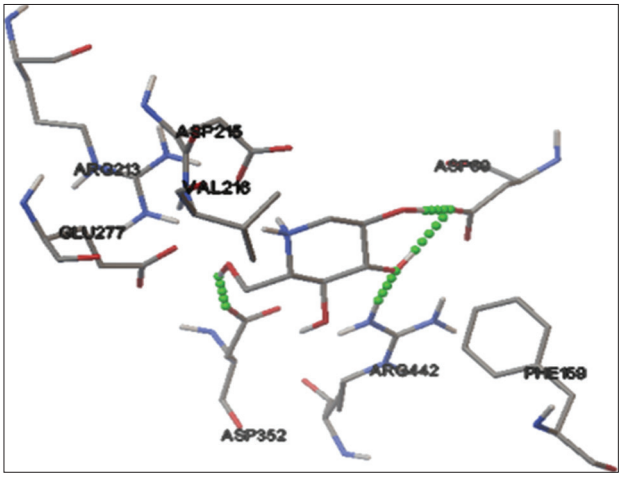

Figure 3: The molecular docking results. The binding conformations of 1-deoxynojirimycin interacting with the active site residues of the modeled *S. cereviseae* α-glucosidase structure

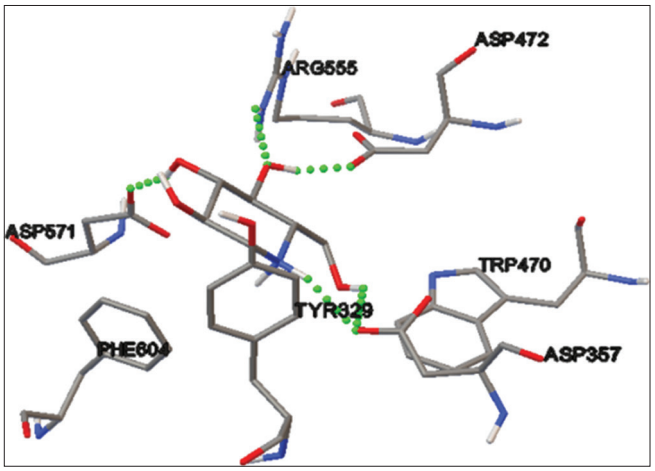

Figure 4: The molecular docking results. The binding conformations of 1-deoxynojirimycin interacting with the active site residues of the modeled *R. norvegicus* α-glucosidase structure

The binding interactions 1-deoxynojirimycin into the active site of *R. norvegicus* modeled protein resulted in energy conformation of −5.93 kkal/mol. The interactions

of the *R. norvegicus* α-glucosidase and 1-deoxynojirimycin proposed in this study were useful to understand the potential mechanisms of the interaction between *R. norvegicus* and 1-deoxynojirimycin. The residues of Asp357, Asp472, Asp571, Trp470, and Arg555 were important for strong hydrogen bonding interaction with 1-deoxynojirimycin, as shown in Figure 4. The binding interactions of acarbose into the active site *R. norvegicus* resulted in the lowest energy conformations of −6.12 kkal/mol. Miglitol and voglibose were considered as moderate IAG and had bonding interactions with α-glucosidase *R. norvegicus*. Bioactivity test for α-glucosidase on rat intestinal used all the four inhibitors such as 1-deoxynojirimycin, acarbose, miglitol, and voglibose as standard references for IAG.

The active site of GANC-human was a pocket formed mainly by the GH31 domain residues such as Asp398, Asp511, Asp587, His645, and Arg571. Residues of Trp472 and Trp509 came into close proximity to the opening of the active site and contributed toward the architecture of the substrate binding site. Additional residues lining the sugar-binding site were Asp511, Trp472, and Trp509. Asp511 acted as the conserved catalytic nucleophile, while Asp587 was highly conserved among GH31 members and making it a likely for acid or base catalyst. Most of GH31 family members had an aromatic residue at the position corresponding to Trp472. In Figure 5, it was shown that the residues of Asp398, Asp511, Asp587, His645, and Arg571 were important for strong hydrogen bonding interaction with 1-deoxynojirimycin.

Docking of 1-deoxynojirimycin into the active site of the GANC human active site resulted in the lowest energy conformations of −6.07 kkal/mol. It had bonding interactions with α-glucosidase GANC human. Acarbose, miglitol, and

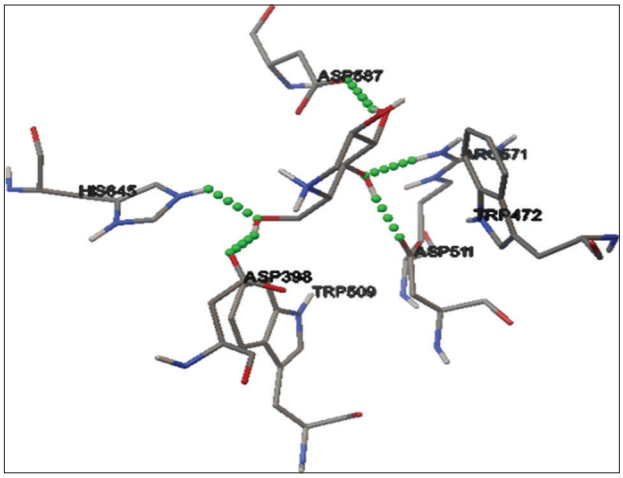

Figure 5: The molecular docking results. The binding conformations of 1-deoxynojirimycin interacting with the active site residues of the modeled GANC-human α-glucosidase structure

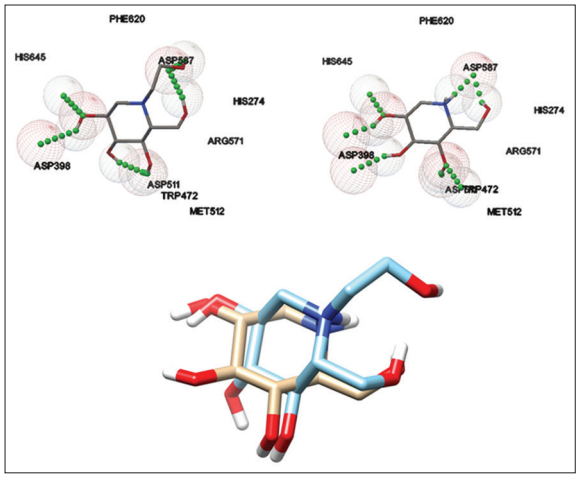

Figure 6: Comparison of the ligand binding pockets with superposed miglitol (a) and 1-deoxynojirimycin (b) of the modeled GANC-human α-glucosidase structure

Table 3: Interaction of the ligan with amino acid residue through molecular docking

Model of α-glucosidase	Ligand	Docking result interaction of the ligand with amino acid residue
S. cerevisiae	Acarbose (1)	Phe159, phe178, Phe303, His280, His351, Asp69, Asp215, Asp307, Asp352 , Arg315, Arg442, Tyr72, Tyr158, Gln279, Gln353, Glu277, Glu411, Val216
	1-Deoxynojirimycin (2)	Phe159, His351, Asp69, Asp215, Asp352, Arg213, Arg442, Glu277
	Miglitol (3)	Phe178, His351, Asp69, Asp215, Asp352, Arg213, Arg442, Glu277, Glu411, Tyr72, Tyr158
	Voglibose (4)	Asp352, Arg315, Arg442, Tyr158, Tyr316, Glu411, Asn415
R. norvegicus	Acarbose (1)	Phe604, Asp233, Asp357, Asp472, Asp571, Arg555, Arg364, Trp435, Tyr329, Gln632, Met473
	1-Deoxynojirimycin (2)	Phe604, Asp357, Asp472, Asp571, Arg555, Trp470, Tyr329, Arg555
	Miglitol (3)	Asp233, Asp571, Arg555, Tyr244, Thr234, Thr235, Met473
	Voglibose (4)	Phe604, Asp233, Asp571, Arg555, Trp435, Tyr329, Met473
GANC human	Acarbose (1)	Phe620, His274, His645, Asp398, Asp587, Arg571, Trp370, Trp472, Thr647, Leu276, Ile621
	1-Deoxynojirimycin (2)	Phe620, His274, His645, Asp398, Asp511, Asp587, Arg571, Trp472, Met512
	Miglitol (3)	Phe620, His274, His645, Asp398, Asp511, Asp587, Arg571, Trp472, Met512
	Voglibose (4)	Phe620, His274, His645, Asp398, Asp511, Asp587, Arg571, Trp472, Met512

voglibose were considered as moderate inhibitors of GANC-human α-glucosidase. Hence, we could see that the use of acarbose would be better, and it was used in conjunction or combination with other drugs.

The active site of *S. cerevisiae* was a pocket, formed by GH31 domain residues such as Asp352 and Arg 442. However, inside of *S. cerevisiae* active site, residues of Gln279, Asp69, Asp215, Asp307, Arg315, His351, Phe159, Phe178, Tyr72, Tyr158, and Glu277 came into close to the opening of the active site and contributed toward the architecture of the substrate binding site. While the active site of *R. norvegicus* was a pocket, molded by GH31 domain residues such as Phe604, Asp357, Asp472, Asp571, Arg555, Tyr329, and Trp470. Moreover, the active site of C-neutral human beings (GANC) was a pocket, builded by GH31 domain residues such as Asp398, Asp511, Asp587, Arg571, and His 645. While, the other residues which contributed toward the architecture of the substrate binding site were Phe620, His645, Asp398, Asp587, Arg572, Met512, and Trp472.

All of the known IAG tested with AutoDock into the active site of modeled protein in 100 docked conformations. The known IAG was docked into the binding pocket of homology model and showed interaction to the important active site residues, as presented in Table 3**.**

Between the four known IAG compounds tested in this study, it could be seen that the 1-deoxynojirimycin had the most excellent bonding interactions with the three models of the protein of α-glucosidase enzyme compared to acarbose, miglitol, or viglibose. Since ΔG of miglitol was quite close to that of 1-deoxynojirimycin in GANC-human, miglitol and 1-deoxynojirimycin had interactions with the residues of the same amino acid residues such as Phe620, His645, His 274, Asp587, Asp398, Asp511, Arg571, Trp472, and Met512. Moreover, they also had four hydrogen bonds with the same amino acid residues such as Asp398, Asp587, Asp511 and His645, as shown in Figure 6**.**

1-Deoxynojirimycin, miglitol, and voglibose inhibitors tended to have relatively similar inhibitory activity for each domain of α-glucosidase. Although it had different affinity binding values, the difference was not very significant. However, the inhibitory activity of acarbose on *R. norvegicus* and GANC-human α-glucosidase was better than on *S. cerevisiae* because the difference affinity binding values were very significant. The chemical structure of acarbose corresponded to that of large tetrasaccharides, whereas the size of 1-Deoxynojirimycin, miglitol, and voglibose corresponded to that of small monosaccharides. The binding affinities of each ligand to domain α-glucosidase reflected ligand size and substrate specificity.[23] Species-based differences in terms of inhibitory activity of acarbose were hypothesized to originate from the binding affinity for *S. cerevisiae*. Given the small size of its binding pocket, *S. cerevisiae* prefered small ligands. The bulky structure of acarbose could not interact well with *S. cerevisiae*. Consequently, acarbose inhibitory activity was lower for the *S. cerevisiae* enzyme than for GANC human and *R. norvegicus*.

CONCLUSIONS

Molecular docking of IAG such as acarbose, 1-deoxynojirimycin, miglitol, and voglibose had been carried out against three models of α-glucosidase protein derived from *S. cerevisiae, R. norvegicus,* and GANC-human. Through molecular docking studies, the model structures of the ligand-receptor complex were obtained. Analysis of the architecture of active site of the three models protein showed differences in their locations. Furthermore, the binding interaction of the inhibitors to the proteins indicated that conserved amino acid residues in the proteins such as *S. cerevisiae*, *R. norvegicus*, and GANC-human played an important role in maintaining a functional conformation and were involved in binding to the inhibitors. The interactions of the proteins and inhibitors in this study were useful to understand the potential mechanism of the interactions between them. Averaged binding affinities of the known glucosidase for three model proteins matched the experimental species differences in terms of inhibitory activity. The low inhibitory activity of acarbose with respect to the *S. cerevisiae* enzyme was caused by the weak interaction of the inhibitor with the *S. cerevisiae* enzyme, which preferred ligands that were smaller than acarbose. The fact that the inhibitory effect of acarbose on the human enzyme was better than to that observed for the *S. cerevisiae* enzyme was explained by a compensation of the charge interactions between human and *S. cerevisiae*. From the four known the IAG compounds tested, it could be seen that the 1-deoxynojirimycin had the most excellent bonding interactions with the three models of the protein α-glucosidase enzyme compared to acarbose, miglitol, and voglibose. GANC-human protein could use as the protein template to find α-glucosidase inhibitor because the main target was human α-glucosidase. The use of GANC was closer to the intended goal target for rational drug design.

ACKNOWLEDGMENTS

We would like to thank the lpdp for their support for this research by giving lpdp funding through BPI Disertation Program. Furthermore, we acknowledge the support from Research Center for Chemistry - Indonesian Institute of Sciences in facilitating the research.

REFERENCES

1. Nashiru O, Koh S, Lee S, Lee D. Novel α -glucosidase from extreme thermophile thermus caldophilus GK24. J Biochem Mol Biol 2001;34:347-54.
2. Bösenberg LH, van Zyl DG. The mechanism of action of oral antidiabetic drugs : A review of recent literature. J Endocrinol Metab Diabetes South Afr 2008;13:80-8.
3. Park H, Hwang KY, Oh KH, Kim YH, Lee JY, Kim K, *et al.* Discovery of novel alpha-glucosidase inhibitors based on the virtual screening with the homology-modeled protein structure. Bioorg Med Chem 2008;16:284-92.
4. Davies G, Henrissat B. Structures and mechanisms of glycosyl hydrolases. Structure 1995;3:853-9.
5. van de Laar FA. Alpha-glucosidase inhibitors in the early treatment of Type 2 diabetes. Vasc Health Risk Manag 2008;4:1189-95.
6. Khan KM, Rahim F, Wadood A, Kosar N, Taha M, Lalani S, *et al.* Synthesis and molecular docking studies of potent α-glucosidase inhibitors based on biscoumarin skeleton. Eur J Med Chem 2014;81:245-52.
7. Liu Y, Zou L, Ma L, Chen WH, Wang B, Xu ZL, *et al.* Synthesis and pharmacological activities of xanthone derivatives as alpha-glucosidase inhibitors. Bioorg Med Chem 2006;14:5683-90.

8. Mehta A, Zitzmann N, Rudd PM, Block TM, Dwek RA. Alpha-glucosidase inhibitors as potential broad based anti-viral agents. FEBS Lett 1998;430:17-22.
9. Fischer PB, Collin M, Karlsson GB, James W, Butters TD, Davis SJ, *et al.* The alpha-glucosidase inhibitor N-butyldeoxynojirimycin inhibits human immunodeficiency virus entry at the level of post-CD4 binding. J Virol 1995;69:5791-7.
10. Pili R, Chang J, Partis RA, Mueller RA, Chrest FJ, Passaniti A, *et al.* The alpha-glucosidase I inhibitor castanospermine alters endothelial cell glycosylation, prevents angiogenesis, and inhibits tumor growth. Cancer Res 1995;55:2920-6.
11. Yamagishi S, Matsui T, Ueda S, Fukami K, Okuda S. Clinical utility of acarbose, an alpha-glucosidase inhibitor in cardiometabolic disorders. Curr Drug Metab 2009;10:159-63.
12. Moorthy NS, Ramos MJ, Fernandes P. A structural analysis of α -glucosidase inhibitors by validated QSAR models using topological and hydrophobicity based descriptors. Chemometr Intell Lab Syst 2011;109:101-12.
13. Park J, Ko S, Park H. Toward the virtual screening of α -glucosidase inhibitors with the homology-modeled protein structure. Bull Korean Chem Soc 2008;29:921-7.
14. Saqib U, Siddiqi MI. 3D-QSAR studies of xanthone derivatives as human α-glucosidase inhibitors CoMFA studies CoMSIA studies. Int J Integr Biol 2009;5:13-9.
15. Saqib U, Siddiqi MI. Probing ligand binding interactions of human α- glucosidase by homology modeling and molecular docking. Int J Integr Biol 2008;22:116-21.
16. Nakamura S, Shimada K, Tanabe G, Muraoka O, Nakanishi I. Computational study on the comparative differences in the activity of inhibitors of human versus rat alpha glucosi dase. Open J Med Chem 2017;7:19-28.
17. Yanuar A. Penambatan Molekule. 1st.ed. Depok: Fakultas Farmasi Universitas Indonesia; 2012.
18. Adisasakwattana S, Chantarashinlapin P, Thammarat H, Yibchok-Anun S. A series of cinnamic acid derivatives and their inhibitory activity on intestinal α-glucosidase. J Enzyme Inhib Med Chem 2009;24:65-9.
19. Kim YM, Wang MH, Rhee HI. A novel α-glucosidase inhibitor from pine bark. Carbohydr Res 2004;339:715-7.
20. Kim YM, Jeong YK, Wang MH, Lee WY, Rhee HI. Inhibitory effect of pine extract on α-glucosidase activity and postprandial hyperglycemia. Nutrition 2005;21:756-61.
21. Jo SH, Ka EH, Lee HS, Apostolidis E, Jang HD, Kwon YI. Comparison of antioxidant potential and rat intestinal α-glucosidases inhibitory activities of quercetin, rutin, and isoquercetin. Int J Appl Res Nat Prod 2010;2:52-60.
22. Nakamura S, Shimada K, Tanabe G, Muraoka O, Nakanishi I. Computational study on the comparative dfferences in the activity of inhibitors of human versus rat alpha glucosidase. Open J Med Chem 2017;7:19-28.
23. Nakamura S, Takahira K, Tanabe G, Muraoka O, Nakanishi I. Homology modeling of human alpha glucosidase catalytic domain and sar study of salacinol derivatives. Open J Med Chem 2012;2:50-60.